International Journal of
Science and Engineering Investigations vol. 9, issue 102, July 2020
Received on July 15, 2020 ISSN: 2251-8843

InAs/GaAs Quantum Dot Superlattice Model for Intermediate Band Solar Cells

H. I. Ikeri[1], A. I. Onyia[2], C. Adjadje[3]
[1,2]Department of Industrial Physics, Enugu State University of science and Technology Enugu, Nigeria
[3]Department of Electrical/Electronics, Estam University of Cotonou Republic of Benin
([1]ifeanyihenry75@yahoo.com)

***Abstract*-**A simplified InAs/GaAs quantum dot superlattice model is presented. Time independent Schrodinger equation and Bloch's theorem were resolved using the Kronig Penney model to determine the band structures. We carried out the numerical simulation using the COMSOL Multiphysics software. From the obtained results we observed an existence of new electronic states (intermediate bands) in the band gap regime. The simulation results reveal that increasing the QD width increases the number of intermediate band IB but lowers its position whereas varying the barrier thickness towards higher values an increase in the IB width was recorded. The intermediate band in solar cell increases photon absorption bandwidth and extends spectral response in the near infra-red region. Thus energy photons less than the fundamental band gap energy can be used to promote electron using the IBs as a stepping stone to create additional optical transition pathways to conduction band. The energy losses due to missed absorption of sub band gap photons in the conventional device is significantly minimized and in principle this contributes to photo current without reducing the open circuit voltage. The extended spectral response to lower energies in InAs/GaAs superlattice indicates a potential route to high operational efficiency.

Keywords- *Intermediate Bands, Bandgap, Quanum Dots, Superlattice, Schrodinger Equation, Kronig Penney Model and Solar Cells*

I. INTRODUCTION

The unique nature of optical and electronic properties of semiconductor superlattice and their extended potential applications in Nano photonic devices covering a broad spectrum has attracted tremendous interest in the emerging field of nanotechnology from both experimental and theoretical viewpoints. Nanotechnology represents an important vehicle to drive the technology of efficient solar cells that will utilize all the wavelengths present in solar spectrum due to quantum effects that prevail at Nano scale regime. One major technology that offers this potential is based on intermediate-band solar cell (IBSC) to increase the efficiency beyond the limit established by Schockley and Queisser through the absorption of sub-band gap photons that otherwise be transmitted in a conventional devices [1].

Solar cells are devices that provide direct conversion of solar energy into electrical energy through photovoltaic PV effect without polluting by-products. They are of great significant for harvesting, development and efficient usage of renewable (green) energy to mitigate the pollution that characterized the use of fossil fuel [2]. The semiconductors are usually the absorbing materials in solar cells. Thus, only photons with specific band gap characteristic of photo absorber can be utilized to promote electron to conduction band. Solar cells of conventional material consist of a single junction semiconductor material [3]. When a photon with energy greater than the band gap of the material strikes the solar cell, it excites an electron with energy exactly equal to the material band gap while the excess energy is lost as heat via lattice vibration [4]. Conversely, energy photons lower than the band gap are transmitted by the material and do not contribute to the photo generated current. If the band gap is lower, solar cell absorbs a larger fraction of the solar spectrum and hence produces a high current but the electrons have lower energy (lower voltage). Also, if the band gap is higher fewer incoming photons can be absorbed but the electrons have higher energy (higher voltage) [5].

These result in a band gap-dependent voltage-current tradeoff. Hence, spectral losses are realized in the conventional solar cells because of the inherent mismatch between the incident solar spectrum and fundamental band gap energy of the absorber material, which places an upper limit on the maximum power conversion efficiency to 31% as calculated by Shockley and Queisser [6]. The solution is none but (a) increasing the photon absorption and (b) reducing the optical losses. These processes are more favorable in QDs due to their combined advantages of discrete electronic states and tunable band gap which confer on them impressive optical and electro-optical behavior suitable for efficient solar cell applications [7]. Thus studies directed at the search for QD-based solar converting devices in which significant increases in solar absorption are observed by alleviating the energy loss effects are of importance [8].

QD superlattice QDSL is an artificial crystal comprising multiple arrays of QDs aligned vertically and horizontally in all

the three spatial dimensions [9]. QDSL has attracted significant attention due to its modified density of state and optical selection rules with controllable electronic states [10]. The confined structure exploits the principle of quantum confinement to engineer carrier states which makes QDs excellent candidates for near infrared IR photo detectors [11]. QDSL technology is proposed as a near term proof of concept to realize an intermediate band solar cell [12]. The biggest advantage of QDs severing as intermediate bands is due to their tunable band gap. The emission and absorption spectrum (QDSL) of are largely determined by the dots width and band gap of the barrier layers. The intermediate band is formed by the array of QDs embedded in a higher band gap (host) material. The QD introduces the discrete electronic states which are theorized to form intermediate band similar to atoms in crystal. The intermediate band represents the energy levels situated within the band gap region of the host material specifically to extend the photon absorption to lower energies (IR) [13].

IBSC has multiple band gaps that cover the whole solar spectrum. In such full spectrum solar cells, the transmission loss is much less than that of a single junction cell [14]. IBSCs use the IB(s) as a stepping stone to promote electrons to CB. In the first step, an electron is launched from the valence band (VB) to the intermediate band (IB), while in the second step; another electron is pumped from the IB to the CB [15]. In this way photons with insufficient energy to promote electrons are absorbed using the ladder approach via transitions from the VB to IB and from IB to CB in addition to conventional valence to conduction bands transitions.

In this paper InAs/GaAs QD superlattice model used in the studies of novel intermediate band solar cells and their performance improvement is formulated.

II. InAs/GaAs Quantum Dot Superlattice Model

The QDs superlattice is based on the resemblance between the QDs and atoms in which QDs play the role of atoms in a real crystal. We recall that a crystalline solid has a regular structure, comprising of periodic array of atoms known as lattice in which the discrete energy levels associated with individual atoms broaden into bands of allowed and forbidden regions. In the same way, if a single QD is an artificial atom then multiple periodic arrays of QDs can be considered an artificial crystal called superlattice with a periodic potential formed by QDs as oppose to atoms in a crystalline material.

The QD superlattice model comprised alternating semiconductors with different band gaps such that smaller band gap semiconductor is sandwiched between two layers of higher band gap materials. The smaller band gap material becomes a potential well while larger band gap materials form potential barriers. Thus two potentials are formed; the well (QDs layer) depth for electrons called conduction band offset due to the difference between the conduction band edges of the well and barrier materials. Similarly the potential depth for holes called valence band offset is formed. In this work, the small band gap semiconductor material considered in the SL is InAs QDs and the larger band gap (barrier) material used is GaAs semiconductor as shown in the Figure 1 below.

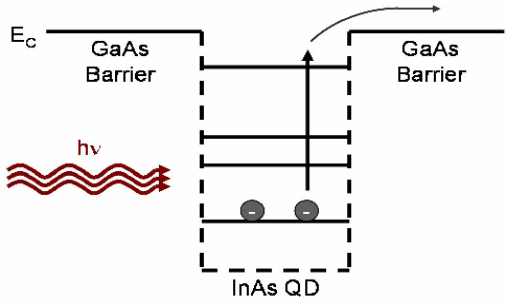

Figure 1. The InAs/GaAs Superlattice Structure

The superlattice assumed in this model is a 3D arrays of cubic InAs QDs embedded in a matrix of GaAs semiconductor to form series of minibands and minigaps along growth direction. The minibands represent energy levels through which electrons can travel thereby extending spectral response beyond the band gap of GaAs in the near infra-red region. The QDs and barrier materials are periodically repeated in space to form a kind of periodic lattice shown in the Figure 2 below.

However we have made the following assumptions:

(i) The confining potential is only conduction band offset and thus the top of the valence band is same both in the barrier and the well material

(ii) The total pumping of electrons from valence band to intermediate band must equate the pumping of electrons from the intermediate band to the conduction band.

(iii) No charge carriers are extracted from the IB, in principle photo generated current can be significantly enhanced without reducing the voltage.

(iv) The IB should be partially filled in order to provide an empty states to receive electron from VB to IB and electron filled state to supply electron from IB to CB

(v) The QD geometry is cubic and arranged in a periodic lattice to establish a well-placed IB boundaries

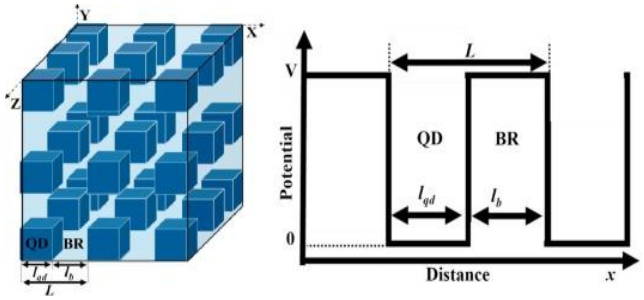

Figure 2. Quantum Dot SupperLattice Diagram

The QDSL structure forms an artificial one-dimensional periodic crystal of finite height with period given as:

$$a = L_Q + L_B \quad (1)$$

where L_Q and L_B represent QD width and barrier thickness respectively. Thus mathematical description and analytical derivation of the energy states of SL is similar to that of 1D crystal lattice which allows us to apply Kronig-Penney model to formulate the dispersion equation which provides the condition for electronic band structures.

The mathematical representation of periodic potential is given as;

$V_{(x)} = 0$ for quantum dot region and $V_{(x)} = V_o$ for barrier region where V_0 is the conduction band offset.

The energies of electrons can be found by solving Schrodinger equations in the two regions. The time independent Schrodinger equations for the motion of electrons along x-direction in both regions are:

$$\frac{d^2\varphi_{(x)}}{dx^2} + \frac{2mE\varphi_{(x)}}{h^2} = 0 \quad (2)$$

for the quantum dot region and

$$\frac{d^2\varphi_{(x)}}{dx^2} + \frac{2m(E-V_0)\varphi_{(x)}}{h^2} = 0 \quad (3)$$

for the barrier region

The Equation 2 and 3 can be expressed respectively as:

$$\frac{d^2\varphi_{(x)}}{dx^2} + k_Q^2\varphi_{(x)} = 0 \quad (4)$$

$$\frac{d^2\varphi_{(x)}}{dx^2} + k_B^2\varphi_{(x)} = 0 \quad (5)$$

where $k_Q^2 = \frac{2mE}{h^2}$ and $k_B^2 = \frac{2m(E-V_0)}{h^2}$

We suppose the general solution to the equations 4 and 5 above are respectively

$$\varphi_{Q(x)} = Ae^{iK_Qx} + Be^{-iK_Qx} \quad (8)$$

$$\varphi_{B(x)} = Ce^{K_Bx} + De^{-K_Bx} \quad (9)$$

where A, B and C, D are the constants in the dot and barrier region respectively and can be obtained by applying the continuous and periodic boundary conditions. If $\varphi_{Q(x)}$ denotes wave function for quantum dot and $\varphi_{B(x)}$ denotes wave function for barrier, these two boundary conditions become:

$$|\psi_1(x)|_{x=0} = |\psi_2(x)|_{x=0} \quad (10)$$

$$\left[\frac{d\psi_1}{dx}\right]_{x=0} = \left[\frac{d\psi_2}{dx}\right]_{x=0} \quad (11)$$

$$|\psi_1(x)|_{x=L_Q} = |\psi_2(x)|_{x=L_B} \quad (12)$$

and

$$\left[\frac{d\psi_1}{dx}\right]_{x=L_Q} = \left[\frac{d\psi_2}{dx}\right]_{x=L_B} \quad (13)$$

For a periodic potential lattice with $V(x+a) = v(x)$, its wave-function satisfies Bloch's theorem of the form:

$$\psi(x) = u(x)e^{ikx} \quad (14)$$

where $u(x+a) = u(x)$ (15)

$$\psi(x+a) = u(x+a)e^{ik(x+a)} \quad (16)$$

thus $\psi(x+L) = \psi(x)e^{ikL}$ (17)

where "a" is the period ($L_Q + L_B$) of the superlattice potential,. Using this, equations 12 and 13 become respectively

$$\psi_1(L_Q) = \psi_2(L_B)e^{ika} \quad (18)$$

and

$$\left[\frac{d\psi_1}{dx}\right]_{x=L_Q} = \left[\frac{d\psi_2}{dx}\right]_{x=L_B} e^{ika} \quad (19)$$

Now applying the boundary conditions in 10, 11, 18 and 19, we obtain the following Equations

$$A + B = C + D \quad (20)$$

$$ik(A-B) = k_B(C-D) \quad (21)$$

$$Ae^{iK_QL_Q} + Be^{-iK_QL_Q} = (Ce^{K_BL_B} + De^{-K_BL_B})e^{iKL} \quad (22)$$

$$ik_QAe^{iK_QL_Q} - ik_QBe^{-iK_QL_Q} = (k_BCe^{K_BL_B} - k_BDe^{K_BL_B})e^{iKa} \quad (23)$$

We now have four homogeneous equations with four unknowns (A, B, C and D). In order to have a non-trivial solution (A = B = C = D = 0) to the above four equations, the determinant of their coefficient must be zero:

$$\begin{vmatrix} 1 & 1 & -1 & -1 \\ ki_Q & -ki_Q & -K_B & K_B \\ e^{iK_QL_Q} & e^{-iK_QL_Q} & -e^{-K_BL_B+iKL} & -e^{K_BL_B+iKL} \\ iK_Qe^{iK_QL_Q} & -iK_Qe^{-iK_QL_Q} & -K_Be^{-K_BL_B+iKL} & K_Be^{K_BL_B+iKL} \end{vmatrix} = 0 \quad (24)$$

By solving and simplifying the 4 x 4 determinant, we obtained:

$$\left(\frac{k_B^2-k_Q^2}{2k_Bk_Q}\right)\sinh(k_BL_B)\sin(k_QL_Q) + \cosh(k_BL_B)\cos(k_QL_Q) = \cos ka \quad (25)$$

In term of energy E, we transform Equ. 25 into

$$\frac{-V_0-2E}{2\sqrt{E(V_0-E)}}\sinh\left[\frac{L_B\sqrt{2m(V_0-E)}}{h}\right]\sin\left[\frac{L_Q\sqrt{2mE}}{h}\right] + \cosh\left[\frac{L_Q\sqrt{2m(V_0-E)}}{h}\right]\cos\left[\frac{L_Q\sqrt{2mE}}{h}\right] = \cos ka \quad (26)$$

The equation 26 is a simple model of dispersion relation for electrons in the QDSL. This is a dispersion relation providing a relationship between the wave number k on the RHS and the energy E on the LHS. In order to produce the solution to the dispersion equation above, we considered first the limiting solution and then general solution as follows.

i. Limiting case in which $V_0 = 0$. We obtained:

$$E = \frac{h^2k^2}{2m} \quad (27)$$

This gives the energies of free electrons in the QD – SL in which there is no limit in the allowed particle energy.

ii. Limiting case in which $V_0 = \infty$

We obtained:

$$E = \frac{n\pi h^2}{8mL^2Q} \quad (28)$$

This gives an expression for the energies of particles in a box and thus the region where no electron is allowed.

iii. General case

We made further simplification and assumed that the product of height and width of the potential barrier $V_o L_B$ be finite and then introduced a dimensionless parameter known as scattering power P**,** which is defined as;

$$P = \frac{mV_0 L_B L_Q}{h^2} = \frac{k_B^2 L_Q L_B}{2} \quad (29)$$

We obtained

$$\frac{P}{K_Q L_Q} \sin k_Q L_Q + \cos k_Q L_Q = \cos kL_Q \quad (30)$$

Equation 30 is a simplified model for the dispersion relation for electron in the QDSL.

III. RESULTS AND DISCUSSION

We present the analytical and simulation results of the theoretical studies based on the models derived in the preceding section. We have solve time independent Schrodinger equation using Kronig- Penney model and applied necessary boundary conditions to calculate the band structures and used COSMOL Multiphysics for numerical simulation. The result obtained considering the first extreme case in which the potential is zero (i.e., V_o = o) reveals that electron energy $E = \frac{h^2 k^2}{2m}$. Here the electrons are free and E represents the kinetic energy only and we have free particle dispersion relation in which there is no limit (gap) on the allowed particle energy as shown in the energy continuum of Fig. 3. In this limit all electrons are free to move without restrictions. The dispersion relation here is parabolic and thus supports classical free electron theory.

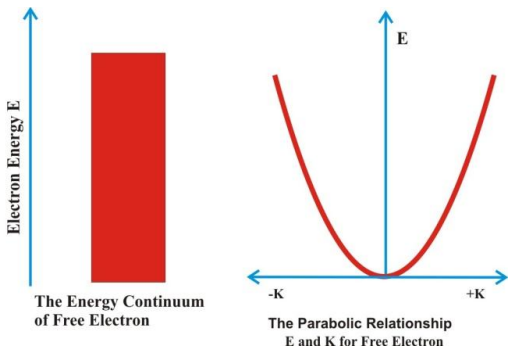

Figure 3. Dispersion Relation and Energy Continuum for Free Electron

In the other extreme in which potential tends to infinity (i.e., $V_o = \infty$) we obtained the energy $E = \frac{n\pi h^2}{8mL^2Q}$, here electrons are constrained and we have the expression for energy levels in an infinite potential well. Hence there will be discontinuity (gap) in the free particle dispersion relation at the boundaries $k_Q = \frac{n\pi}{L_Q}$ and this manner we get series of discontinuities in the dispersion relation for all other k values as shown in the Figure 4.

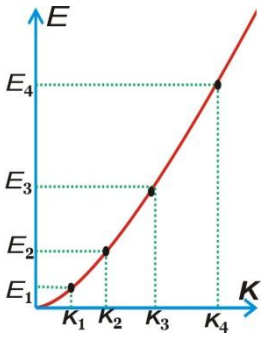

Figure 4. Dispersion Relation of Confined Electron and Free Electrons

The black dots represent the energy of particle in a box and the red line the free particle energy. However, both depend upon wave vector in similar manner but the particle in a box assumes discrete energy levels.

In the general case the simplified model obtained is $\frac{P}{K_Q L_Q} \sin k_Q L_Q + \cos kL_Q = \cos kL_Q$. This model describes the motion of electron with periodic motion and provides a definite relationship between the energy E through k_Q on the LHS and the wave vector k on the RHS. This is therefore a dispersion relation for electrons in the QDSL which provides condition on the allowed energies of the electrons in the periodic structure. If the LHS of the Equation is expressed as $F(E)$, we have $F(E) = \cos kL_Q$. It is clear trigonometrically that for a solution to exist, $\cos kL_Q$ can only take values between -1 and 1 and the values of kL_Q on these limits are respectively 0 and $\frac{\pi}{a}$.

It follows that the function on the LHS is bounded in the region [-1, 1] since it is equal to $\cos kL_Q$. This imposes limit on the amount of k. This in turn means there are values of k_Q for which valid k values occur (solution exists) and energies corresponding to this k_Q values are allowed. Also, there will be some values of k_Q which there are no real values of k and hence no proper solution exists, in which case there will be forbidden gap in the spectrum of energies. That is, if energy E is in the allowed energy region the Schrodinger equation for the SL has a solution and if E is not in an allowed energy band there is no solution. A plot of $F(E)$ as a function of energy is shown in the Figure 5.

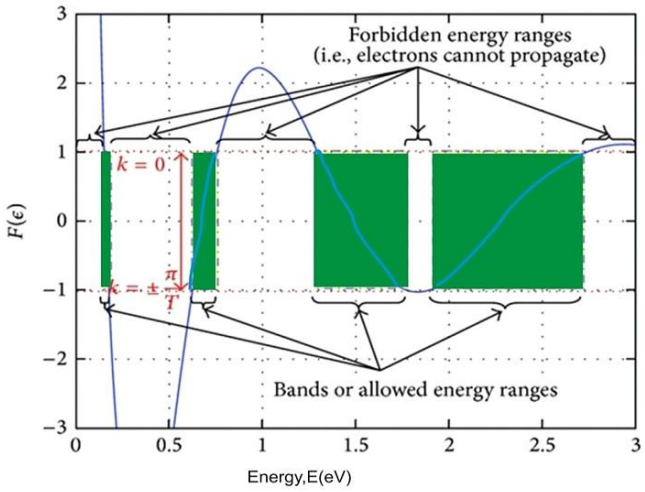

Figure 5. F(E) versus E

The dispersion curve is thus characterized by the bands of allowed energy separated by the disallowed energy bands (forbidden region) similar to that of conventional band structure. The difference between the proposed models to that of the conventional case is that our model is artificial material and the energy band can be controlled by varying the width of different layers. In other words for real value of k the magnitude of $\cos kL_Q$ should be less than 1 which corresponds to the allowed energy band, also the value of energy for which $\cos kL_Q$ is greater 1, only the imaginary values of k are possible which correspond to the forbidden regions as shown in the Figure 6 blow:

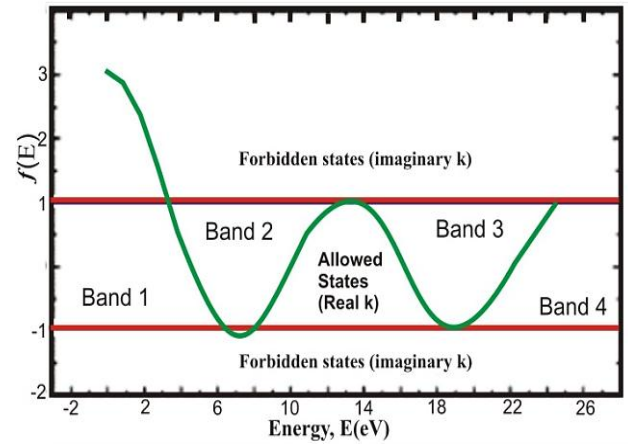

Figure 6. F(E) versus E

The appearance of energy bands spectrum separated by forbidden regions (gaps) is the hallmark of periodic potential. This was as a result of the additional periodic potential provided by the conduction band offset which causes the continuous energy band of the conduction band to be splited into allowed and forbidden regions. This new set of the allowed region are called mini bands as their width are much smaller than that of original conduction band. The reason for this is attributed to the fact that the superimposed potential has much larger period than the period of the host crystalline and thus gives rise to smaller brilliant zones. These mini bands constitute energy levels where electrons can easily travel through the crystal. The collection of this electron bands within the semiconductor band gap leads to the effective intermediate band IB

The following facts are ascertained from the dispersion result:

- The energy spectrum of electrons in the superlattice consists of an infinite number of allowed energy bands separated by intervals in which there are no allowed energy levels otherwise known as band gaps.
- As energy E increases the allowed energy bands increase in width and so the width of forbidden energy region becomes narrower.
- The width of the allowed energy states for electrons decreases with increasing value of P while the forbidden energy gap moves to higher energies.

Following the fundamental relation $F(E) = \cos kL_Q$, we generated a vital figure known as dispersion diagram showing the energy versus wave number (E vs k). To generate the dispersion diagram we started at E = 0 and computed $F(E)$, if $F(E) = |\cos kL_Q| > 1$ we are in a band gap (forbidden energy band) and if we increase the energy a bit such that $|F(E)| \leq 1$ we are at allowed energy band and this corresponds to $k = \frac{1}{L_Q}\cos^{-1} F(E)$, since cosine is an even function it implies –k will also be a solution. By increasing E continuously by small values we have series of allowed and forbidden energy bands as illustrated in the E (k) curve shown in the Figure 7 in the extended zone scheme.

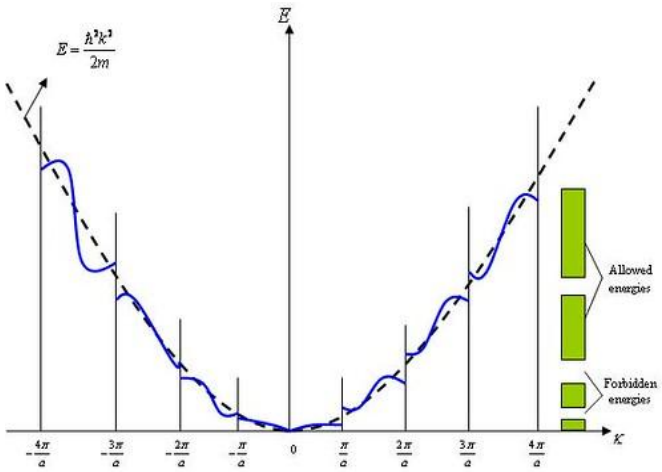

Figure 7. Energy Verses Wave Vector Showing the Gaps that appear when ka = n$\boldsymbol{\pi}$

The broken lines represent the points $k = \frac{n\pi}{a}$ where the curve is discontinuous and marks the forbidden region. The curve indicates that the group velocity (slope) $v_g = \frac{dE}{dK}$ will varnish at the boundaries which shows that there is no propagation and the electron momentum is confined within the allowable k. The allowed region or zone ranging from $\frac{-\pi}{a}$ to $\frac{\pi}{a}$ is the first Brillouin zone. Following the discontinuity another allowed region extended to $\frac{-2\pi}{a}$ to $\frac{\pi}{a}$ and $\frac{2\pi}{a}$ to $\frac{\pi}{a}$. This is the second Brillouin zone. In the same manner subsequent Brillouin zones continue in consistence with Bragg's condition that band gap occurs whenever $k = \frac{n\pi}{a}$ for any non-zero integer n, of an electron moving along one dimensional crystal of period a.

IV. Intermediate Band Solar Cells IBSCs

IBSCs are novel concept in solar cell technology in which sub band gap energy photons can promote electron to conduction band using intermediate band IB as ladder. The IBSCs are specifically designed to tackle the problem of transmission losses associated with photon energies below the material band gap via extension of the spectral response to near infra-red (lower energies) region. The absorption of low energy photons that are usually lost in the conventional cells provides increased photo current while the higher band gap material maintains higher voltage. Thus the output power which the product of photo current and open circuit voltage will be substantially improved.

V. One Intermediate Band Solar Cell

This is a solar cell that uses one intermediate band IB in between the band gap region of semiconductor to produce 3 bands semiconductor structure. By careful observations we have ascertained in this work that if there are n intermediates bands the total upward energy transitions T in the IBSC is calculated using the permutation relation T = ${}^{N}_{n}P$ where n is total number of IB(s) and N the sum of valence band, conduction band and intermediate band(s). Thus for one intermediate band the total upward energy transition is calculated as:

$$T = \frac{3!}{(3-1)!} = 3$$

It means for one IB there will be three optical upward energy transitions which are transitions from VB to IB, from IB to CB and the conventional VB to CB. In this way the solar photons with low energy to pump electrons from the valence to the conduction band can use this intermediate band concept as a stepping stone (ladder approach) to optically generate electron hole pair. Thus by absorption of photon in this device three optical absorption and transitions are possible. The three absorption processes are denoted by α_1, α_2 and α_3 respectively as shown in the Figure 8b. The fundamental relationship between the absorption coefficients corresponding to different energies is as shown in the Figure 8a.

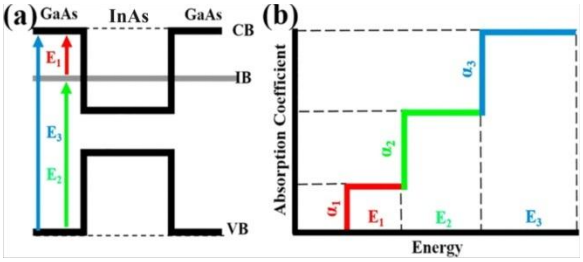

Figure 8. Intermediate band formed by QDSL and the Three Absorption Processes

The first sub band gap photons with energy, $E = h\omega 1$ which usually transmitted in the conventional device are absorbed through transition from valence band to intermediate band (which has an empty state to receive this electron), and the second low energy photons $E = h\omega 2$ are also absorbed through transition from intermediate band (which also has filled state to supply electron) to conduction band and the third conventional solar photons $E = h\omega 3$ which is a usual direct transition from valence band to conduction band shown in the Figure 9.

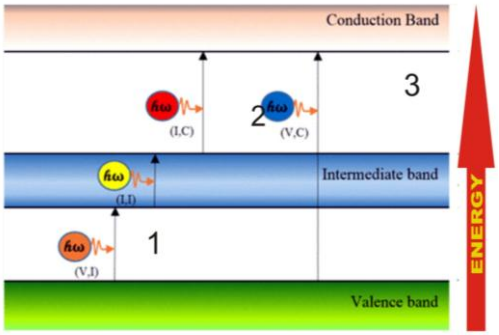

Figure 9. One Intermediate Band Solar Cell Mechanism with the possible Electronic Transitions

VI. Two Intermediate Bands Solar Cells

These are solar cells characterized by the existence of a two IBs located in the forbidden region of semiconductor. In this way 4-band semiconductor structure is formed and the total number of upward energy transitions in this device based on the above model is calculated as:

$$T = \frac{4!}{(4-2)!} = 6$$

This means that in an IBSC made up of two IBs there are six upward energy transitions which are E1: transition from VB to IB1, E2: transition from IB1 to IB2, E3: transition from IB2 to CB, E4: transition from IB1 to CB and the conventional VB to CB (bandgap) transition which also implies six optical absorption possibilities as shown in the Figure 10. It follows

that increase in the number of IBs increases the absorption possibilities which in turn provides significant increase in the conversion efficiencies through increase in the photo generated current.

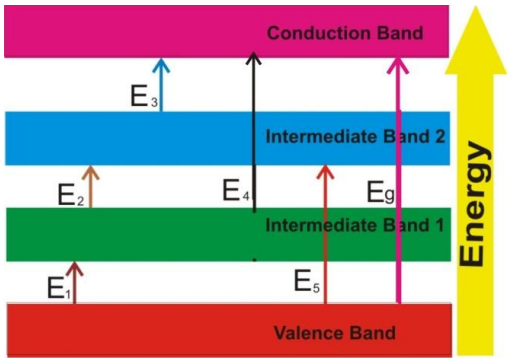

Figure 10. Two Intermediate Band Solar Cell Mechanism with the possible Electronic Transitions

Intermediate band solar cell has shown great potential to enhance light absorption in a single junction cells. The photo generated current will be greater than the current that would be ordinarily generated by conventional cell without an intermediate band. In this way the efficiency is increased beyond the so called upper limit.

VII. CONCLUSION

A theoretical study on the influence of intermediate electronic bands (IBs) on the performance of the solar cell is theoretically presented. We have carried out the numerical simulation using the COMSOL Multiphysics software. From the obtained results we observed the existence of mini bands and mini gaps in the band gap regime of host material. The mini bands constitute IB(s) where electrons can easily travel through the crystal. It is found that the position of IBs can be controlled by varying the QDs width and whereas, width of IB can be controlled by varying the barrier thickness. The intermediate band produces an extended spectral response to lower energies. Thus current loss due to missed absorption of low band gap photons in the conventional device is minimized which dramatically increase the amount of photo generated current without sacrificing the open circuit voltage.

REFERENCES

[1] Nozik, A.J. (2006). 'Chapter 15 - Quantum Structured Solar Cells'. In: Nanostructured Materials for Solar Energy Conversion. Ed. by Tetsuo Soga. Amsterdam: Elsevier, pp. 485–516.

[2] Jabbour, G. and Doderer, D. (2010).Quantum Dot Solar Cells. *Nat. Photonics*,4: 604-605

[3] Ikeri H. and Onyia A. Investigation of Optical Characteristics of Semiconductor Quantum Dots for Multi Junction Solar Cells Applications. Intl Jol of Scientific and Technological Research Vol. 8, Issue 10, Oct., 2019

[4] Nozik, A.J. (2001). Spectroscopy and hot electron relaxation dynamics in semiconductor quantum wells and quantum dots. *Annu. Rev. Phys. Chem*. 52:193-231.

[5] Sergon, E. (2012). Colloidal Quantum Dot Solar Cells. *Nat. Photonics*, 6: 133-135.

[6] Shockley, W. and Queisser, H.J.(1961). Detailed Balance Limit of Efficiency of *p-n* Junction Solar Cells. *J. Appl. Phys.*, 32: 510 – 520

[7] Nozik, A.J. (2003). The Next Generation Photovoltaics, High Efficiency through Full Spectrum Utilization. Edited by Martí A, Luque A, Institute of Physics, Bristol, UK. pp. 196-222

[8] Nozik, A.J. (2010). Nanoscience and Nanostructures for Photovoltaics and Solar Fuels. *Nano Lett*., 10: 2735-2741.

[9] Wasilewski, Z. R. (1999).Size and shape engineering of vertically stacked self-assembled quantum dots J Crystal Growth, 201-202 Supplement C.

[10] Liu, J. L. (1999).Observation of inter-sub-level transitions in modulation-doped Ge quantum dots Appl Phys Lett, 75 (12)

[11] Bayer, M. (2001).Coupling and entangling of quantum states in quantum dot molecules Science, 291 (5503)

[12] Imran, A. (2018).Numerical modelling of high efficiency InAs/GaAs intermediate band solar cell Int Conf Opt Instrum Technol, 10622.

[13] Lacarenkova, O. L. (2005). Miniband Formation in QD crystal. Journal of Applied Physics, 89(10), pp 5509-5515.

[14] Luque, A., Martí, A., López, N., Antolín, E., Cánovas, E., Stanley, C., Farmer, C., Caballero, L.J., Cuadra, L. and Balenzategui, J.L. (2005). Experimental analysis of the quasi-Fermi level split in quantum dot intermediate-band solar cells. *Appl. Phys. Lett*. 87: 083505-083508.

[15] Luque A., and Marti A. (2010). The Intermediate Band Solar Cell Progress Toward The Realization of an Attractive Concept. *Advanced Materials*, 22: 169 – 174.

[16] Yeda A.(2017).The Effects of Interdot Spacing and Dot Size on the Performance of InGaAs/GaAs QDIBSC. *International Journal of Photoenergy*, vol. 2017.

How to Cite this Article:

Ikeri, H. I., Onyia, A. I., Adjadje, C. (2020). InAs/GaAs Quantum Dot Superlattice Model for Intermediate Band Solar Cells. International Journal of Science and Engineering Investigations (IJSEI), 9(102), 73-79. http://www.ijsei.com/papers/ijsei-910220-10.pdf